Transition State Dynamics of $Ar_n(ClHCl)$ ($n = 0-5$): Effects of Complex Formation on the Dynamics and Spectroscopy

Holly B. Lavender and Anne B. McCoy*

Department of Chemistry, The Ohio State University, Columbus, Ohio 43210

Received: August 25, 1999

The effects of intermolecular interactions on the transition state dynamics of the Cl + HCl reaction are investigated through time-dependent quantum simulations of the evolution of the ground state wave function for $Ar_n(ClHCl^-)$ on the $Ar_n(ClHCl)$ potential when $n = 0-5$. A reduced dimensional approach has been employed in which the quantum/semiclassical time-dependent self-consistent field (Q/SC TDSCF) approximation is used to propagate the dynamics of the hydrogen and chlorine atoms, respectively, while the argon atoms are constrained to remain in the equilibrium configuration in $Ar_n(ClHCl^-)$. Analysis of the wave functions, obtained from these simulations, shows that as more argon atoms are introduced there is a change in the short time dynamics. When no argon atoms are present, the hydrogen atom rotates off of the Cl−Cl axis. As the number of argon atoms is increased, this motion becomes blocked, and when four or five argon atoms are present, the Cl−H−Cl subsystem is constrained to dissociate collinearly. This change in the dynamics of the hydrogen atom is reflected in an increase in the amount of energy that is transferred to the chlorine atoms as n is increased. It also results in qualitative changes in the calculated photoelectron spectra of $Ar_n(ClHCl^-)$.

Introduction

An important issue in chemistry involves understanding the effects of solvation on chemical reaction dynamics. Over the past several decades, experimental and theoretical approaches have developed significantly, and a variety of atom plus diatom (A + BC) reactions have been mapped out very accurately.[1−5] While much can be learned from these studies most chemistry, whether in the laboratory or in nature, does not take place in a vacuum but in solvated environments. An important first step in the overall goal of understanding the effects of solvation on chemical reaction dynamics comes in understanding how the dynamics of a simple system, evolving from reactants to products, is affected by the presence of a small number of chemically inert atoms or molecules. In the present study, we focus on the Cl+HCl reaction and, in particular, how the evolution of a wave packet off of the transition state region of the potential is affected by the introduction of one to five argon atoms.

Our motivation for studying the dynamics of the $Ar_n(ClHCl)$ ($n = 0-5$) system comes from a variety of experimental studies in which the photoelectron spectrum of a suitable anion is used to probe the transition state dynamics of the corresponding neutral system.[6−14] In addition to investigating the transition state dynamics of a variety of bimolecular reactions, including the Cl + HCl reaction,[7,8] Neumark and co-workers have studied changes in the photoelectron spectra of IHI^- and I^- upon clustering with rare gas atoms, N_2O or CO_2.[12−14] Although the $Ar_n(ClHCl)$ system has not been studied experimentally by these methods, the abundance of empirical and ab initio information about the potential surfaces for $Ar_n(ClHCl)$ and $Ar_n(ClHCl^-)$ make these systems ripe for theoretical investigations.[15−19] A variety of approaches have been employed to study the transition state dynamics of ClHCl.[20−25] In the present study we use time-dependent wave packet techniques. Further, due to the high dimensionality of these systems, the dynamics is propagated using the quantum/semi-classical time-dependent self-consistent field (Q/SC TDSCF) approximation.[26−29]

We focus on how the dynamics and spectroscopy of ClHCl change as the number of argon atoms is increased from zero to five. Previous studies of the transition state dynamics of the ClHCl system show that the initial decay of the wave function off the transition state primarily involves rotation of the hydrogen atom out of the center of the Cl−Cl axis.[25] We have found that the introduction of an argon atom has little effect on the transition state dynamics or spectroscopy.[30] This result reflects the fact that the argon atom perturbs only a small fraction of the configuration space that is sampled by the hydrogen atom. As more argon atoms are introduced, a larger fraction of configuration space will be affected, and in the case of the system with five argon atoms, the ClHCl subsystem is fully encircled by argon atoms.[29] In this case, the hydrogen atom will be confined in the region between the chlorine atoms during the initial stages of the dissociation process and will be constrained to dissociate colinearly. In this paper, we will investigate how the transition state dynamics and spectroscopy of the Cl+HCl reaction evolve as one to five argon atoms are introduced.

System

Potential Functions. To simulate the transition state dynamics of the Cl+HCl reaction, the potential surfaces for $Ar_n(ClHCl)$ and $Ar_n(ClHCl^-)$ need to be constructed. As in our previous work, we approximate these potentials by pair-wise sums of empirically determined interactions.[30] This approach has the advantage that, while only the most important many-body interactions are included, we are using the best available description of the important two-body interactions.

* Corresponding author. Email: mccoy@chemistry.ohio-state.edu.

10.1021/jp993027h CCC: $19.00
Published on Web 12/23/1999

We approximate the $Ar_n(ClHCl)$ intermolecular potential by

$$V^{inter}_{Ar_n(ClHCl)}(\mathbf{R}) = \sum_{i=1}^{n}[V^{M}_{ArH}(R_{Ar_iH}) + V^{M}_{ArCl}(R_{Ar_iCl_1}) + V^{M}_{ArCl}(R_{Ar_iCl_2})] + \sum_{j>i} V^{L-J}_{ArAr}(R_{Ar_iAr_j}) \quad (1)$$

where R_{XY} represents the distance between atoms X and Y. We represent the Ar−ClHCl interactions as a sum of Morse oscillators:

$$V^{M}_{ArX}(R_{Ar_iX}) = D^{X}_{e}\{1 - \exp[-\alpha^{X}(R_{Ar_iX} - R^{e}_{ArX})]\}^2 \quad (2)$$

with X = H or Cl. The parameters that are used in these potentials can be found in Table 3 of ref 30.[50] The interactions among the argon atoms are represented by a Lennard-Jones potential:

$$V^{L-J}_{ArAr}(R_{Ar_iAr_j}) = 4\epsilon\left[\left(\frac{\sigma}{R_{Ar_iAr_j}}\right)^{12} - \left(\frac{\sigma}{R_{Ar_iAr_j}}\right)^{6}\right] \quad (3)$$

with σ = 3.359 Å and ϵ = 99.51 cm^{-1}.[31] Finally, the total potential for the $Ar_n(ClHCl)$ system is obtained by adding the LEPS potential for the Cl + HCl reaction given by Bondi et al. to $V^{inter}_{Ar_n(ClHCl)}$.[15]

The basic structure of the $Ar_n(ClHCl^-)$ potential is identical to that for $Ar_n(ClHCl)$, with a harmonic $ClHCl^-$ potential[17] substituted for the ClHCl LEPS surface. In addition, we must consider the effects of charge on the intermolecular interactions. In constructing these contributions to the potential, we assume that each of the chlorine atoms carries a $-1/2$ charge. This leads to[19,32]

$$V^{inter}_{Ar_n(ClHCl^-)}(\mathbf{R}) = V^{inter}_{Ar_n(ClHCl)}(\mathbf{R}) - \frac{\alpha_{Ar}}{2}\sum_{i=1}^{n}\left[\left(\frac{\partial\varphi_i}{\partial x_i}\right)^2 + \left(\frac{\partial\varphi_i}{\partial y_i}\right)^2 + \left(\frac{\partial\varphi_i}{\partial z_i}\right)^2\right] + \sum_{k=1}^{2}\sum_{j>i}^{n}\frac{\mu^{(k)}_{Ar_i}\mu^{(k)}_{Ar_j}}{R^3_{Ar_iAr_j}}(2\cos\theta_{ijk}\cos\theta_{jik} + \sin\theta_{ijk}\sin\theta_{jik}) \quad (4)$$

In the second term, α_{Ar} is the polarizability of argon (11.096 a_0^3),[33] (x_i,y_i,z_i) represents the Cartesian coordinates of the ith argon atom, and[32]

$$\varphi_i = -\frac{1}{2}\left[\frac{1}{|\vec{R}_{Ar_iCl_1}|} + \frac{1}{|\vec{R}_{Ar_iCl_2}|}\right] \quad (5)$$

The third term in eq 4 reflects the fact that charges on the chlorine atoms induce a dipole moment on each of the argon atoms. The induced dipole is given by[19]

$$\mu^{(k)}_{Ar_i} = -\frac{\alpha_{Ar}}{2R^2_{Ar_iCl_k}} \quad (6)$$

and θ_{ijk} represents the $Ar_i-Ar_j-Cl_k$ angle.

Coordinates and Hamiltonian. We use the mass weighted normal coordinates of the $Ar_n(ClHCl^-)$ complexes in our simulations of the transition state dynamics of $Ar_n(ClHCl)$. The equilibrium geometries of the $Ar_n(ClHCl^-)$ and the four largest calculated harmonic frequencies are reported in Table 1.

TABLE 1: Initial Geometries and Frequencies for the $Ar_n(ClHCl^-)$ Complexes

parameter	$n=0$	$n=1$	$n=2$	$n=3$	$n=4$	$n=5$
R_{HCl} (Å)	1.5716	1.5711	1.5706	1.5701	1.5699	1.5691
R_{ArH} (Å)		3.1997	3.2067	3.2015 3.2152[a]	3.1726	3.2086
θ_{ClHCl} (deg)	180.00	179.15	179.98	178.70	180.00	180.00
θ_{ArHAr} (deg)			72.7	72.5	90.0	72.0
ω_{Cl} (cm^{-1})	309	310	310	310	311	311
ω_{H_x} (cm^{-1})	791	789	804	830	838	840
ω_{H_y} (cm^{-1})	791	815	819	813	838	840
ω_{H_z} (cm^{-1})	768	767	765	764	761	761
D_e (cm^{-1})[b]	0	744	1569	2215	3143	4116
E_{sh} (eV)[c]	0.000	0.0802	0.1592	0.2143	0.3177	0.3829

[a] Distance for the central argon atom. [b] $D_e = E(n\text{Ar} + (\text{ClHCl})^-) - E(\text{Ar}_n(\text{ClHCl})^-)$. [c] The position of the origin of the transition state spectrum of $Ar_n(ClHCl)$, measured relative to the origin when $n = 0$.

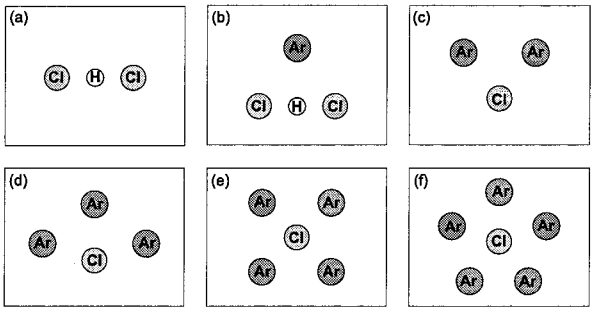

Figure 1. Minimum energy geometries for $Ar_n(ClHCl^-)$ clusters for (a) $n = 0$, (b) $n = 1$, (c) $n = 2$, (d) $n = 3$, (e) $n = 4$, and (f) $n = 5$. The argon atoms are in the *xy* plane, with the *z*-axis defined to be along the Cl−H−Cl axis. In all cases, the complexes are symmetric with respect to reflection in the *yz* plane.

The minimum energy geometries of the $Ar_n(ClHCl^-)$ clusters are sketched in Figure 1. When $n = 0$, $ClHCl^-$ is linear with the hydrogen atom located at the center of the Cl−Cl axis.[17] When one argon atom is introduced, the cluster is approximately T-shaped,[30] while in the cluster with five argon atoms, the argon atoms form a regular pentagon in the plane perpendicular to the ClHCl axis, centered on the hydrogen atom.[29] The minimum energy geometries of the clusters with one, two, and three argon atoms are similar to the structures that would result when four, three, or two argon atoms are removed from a cluster that contained five argon atoms. This result is reflected in the similarity in the Ar−H distances in these four clusters as well as the near 72° Ar−H−Ar bond angles in the clusters with two or three argon atoms. In the case of the cluster with four argon atoms, the minimum energy structure corresponds to the argon atoms forming a square around the center of the ClHCl axis, and the Ar−H distances are 0.03 Å smaller than those observed in the other clusters.

The observed differences between the structure of the complex with four argon atoms and the other four complexes studied here reflect the competition between the attractive Ar−Ar interaction from the Lennard-Jones potential in eq 3 and the repulsive interaction between induced dipoles on the argon atoms. In addition, there is a competition in the attractive interactions between minimizing the individual Ar−Ar interaction energies and maximizing the number of nearest neighbors. For $n = 2$ or 3 the individual Ar−Ar interactions are minimized, whereas when $n = 4$ the repulsive induced dipole-induced dipole interactions becomes more important. In the case of $n = 5$, the three considerations lead to similar structures, making this a particularly stable cluster size. This result is also reflected in the dissociation energies reported in Table 1.

Finally, we find that there is a slight decrease in the H−Cl bond distance as the number of argon atoms is increased, as well as a slight increase in the Ar−H distance in all but the $Ar_4(ClHCl^-)$ cluster. The decrease in the HCl distances reflects an increase in the total number of Ar−Cl interactions, the minimum of which is at shorter Ar−Cl distances than are achieved in the Ar($ClHCl^-$) complex. This factor also causes the ClHCl to bend slightly when $n = 1$, 2, or 3. The increase in the Ar−H distances reflects a competition between minimizing the Ar−Ar interactions and the much weaker Ar−H interactions.

For each of the cluster sizes, there are $3N - 6$ normal modes, where N is the number of atoms. Of these, three correspond to the motions of the hydrogen atom and one to the Cl−Cl stretch. The remaining $3N - 10$ normal modes correspond to motions of the argon atoms. Given the factor of 40 difference between the masses of hydrogen and argon or chlorine and the difference between the strength of the ($ClHCl^-$) intramolecular interactions and those with and among the argon atoms, the resulting normal modes can be divided into three frequency regimes.

There are three frequencies between 750 and 850 cm^{-1}, ω_{H_x}, ω_{H_y}, and ω_{H_z}, that correspond to the motions of the hydrogen atom along the three Cartesian axes. For all cluster sizes, ω_{H_z} is the smallest of the three frequencies and corresponds to motion of the hydrogen atom along an axis that is parallel to the Cl−Cl axis. The two higher frequency modes correspond to motions of the hydrogen atom perpendicular to this axis. When $n = 0$, 4, or 5, these two frequencies are equal. This is a reflection of the fact that $ClHCl^-$ is linear in the equilibrium configuration of these clusters. In the clusters with one and two argon atoms, ω_{H_y} is larger than ω_{H_x}. This reflects the fact that because the argon atoms lie in the half plane with $y > 0$, they will have a large effect on the motions of the hydrogen atom in this direction. On the other hand, motion of the hydrogen atom along the x-axis will be much less strongly affected by the presence of the argon atoms. This trend is reversed when there are three argon atoms. As can be seen in Figure 1c, in this case one of the argon atoms lies on the y-axis while the other two lie 17.3° above the xz plane. As such, motion along the x-axis will be more strongly affected by the presence of the argon atoms than motion along the y-axis.

The next highest frequency regime is at 309 cm^{-1}, and contains only one frequency, ω_{Cl}. This frequency is much less sensitive to the complex size than the three higher frequencies as it corresponds to the Cl−Cl stretching vibration. The remaining frequencies are all smaller than 100 cm^{-1} and correspond to motions of the argon atoms. As these motions are essentially decoupled from those of the hydrogen and chlorine atoms over the short times of interest in the present study, we have set these normal mode coordinates to zero in our simulations of the transition state dynamics of $Ar_n(ClHCl)$.

One advantage to using normal coordinates is that the kinetic energy contribution to the vibrational Hamiltonian takes on a simple form if we neglect the small contributions from vibrational angular momentum and the Watson term.[34] In other words, for a system with $3N - 6$ vibrational degrees of freedom $\{q_j\}$, the ($J = 0$) Hamiltonian then becomes

$$\hat{H} = \sum_{j=1}^{3N-6} \frac{\hat{p}_j^2}{2} + V(\mathbf{q}) \tag{7}$$

Methods

The TDSCF Approximation. Previous studies on this and similar systems have shown that the TDSCF approximation provides a valuable tool for studies of the molecular dynamics of systems where a full quantum mechanical treatment are computationally intractable.[25,27,29,35−39] The TDSCF approximation has been described in detail elsewhere, so only a brief description will be given here.

In the most general form of the TDSCF approximation, the wave function that describes a system with M vibrational degrees of freedom can be approximated by a product of one-dimensional wave functions:

$$\Psi^{\mathrm{TDSCF}}(\mathbf{q};t) = \sum_{j=1}^{M} \psi_j(q_j;t) \exp\left(i \frac{M-1}{\hbar} \int_0^t \langle V \rangle(t')\mathrm{d}t' \right) \tag{8}$$

where q_j is the jth normal mode coordinate in which the system is propagated, and $\langle V \rangle(t')$ is the expectation value of the potential, averaged over $\Psi^{\mathrm{TDSCF}}(\mathbf{q};t')$.

These one-dimensional wave functions are propagated using the time-dependent Schrödinger equations:

$$i\hbar \frac{\partial \psi_j}{\partial t} = \hat{H}_j^{\mathrm{SCF}} \psi_j \tag{9}$$

where

$$\begin{aligned} \hat{H}^{\mathrm{SCF}} &= \frac{\hat{p}_j^2}{2} + \langle \prod_{k \neq j} \psi_k | V | \prod_{k \neq j} \psi_k \rangle \\ &= \frac{\hat{p}_j^2}{2} + V_j^{\mathrm{eff}}(q_j,t) \end{aligned} \tag{10}$$

A complicating issue in these calculations comes from the time dependence of V_j^{eff}. As in previous studies,[25] we approximate this time dependence by propagating the one-dimensional wave functions over a series of short time intervals $t \rightarrow t + \Delta t$, where Δt is chosen so that the V_j^{eff} are approximately constant over each time step. In the present study, we use $\Delta t = 1$ au, or approximately 0.025 fs.

Because we are focusing on the short time transition state dynamics of the Cl+HCl reaction, with total propagation times of no more than 72 fs, the most important couplings in the system are among the coordinates that describe the position of the hydrogen atom. In our previous work on the ClHCl system we found that the simple TDSCF approximation, described above, is inadequate, even for the relatively short propagation times studied here. The approximation can be improved dramatically if Ψ^{TDSCF} in eq 8 is approximated by the product of a wave function that is a function of the three coordinates that describe the motions of the hydrogen atom $\mathbf{q}_H$ and a set of one-dimensional wave functions that are functions of each of the remaining coordinates.[25,40] This allows us to treat the important couplings among the coordinates that describe the motions of the hydrogen atom exactly, while approximating the couplings between these coordinates and those that involve the heavy atoms. Further, due to the relatively weak couplings between the motions of the argon atoms and those of the ClHCl subsystem, we have frozen the positions of the argon atoms and Ψ^{TDSCF} is approximated by

$$\Psi^{\mathrm{TDSCF}}(\mathbf{q};t) = \chi(q_{H_x},q_{H_y},q_{H_z};t)\phi(q_{Cl};t)\exp\left(\frac{i}{\hbar}\int_0^t \langle V \rangle(t')\mathrm{d}t'\right) \tag{11}$$

where q_α represents the normal mode coordinate that corresponds to ω_α in Table 1.

In this formulation of the TDSCF approximation, we propagate a three-dimensional and a one-dimensional time-dependent wave packet, rather than four one-dimensional ones. We make the additional approximation that, because the mass of chlorine is 35 times that of hydrogen, $\phi(q_{Cl};t)$ can be propagated semiclassically, while $\chi(\mathbf{q}_H;t)$ is propagated quantum mechanically. Previous studies of the ClHCl system have shown that such a quantum/semiclassical TDSCF (Q/SC TDSCF) treatment can be performed without significant loss of accuracy compared to the quantum/quantum treatment.[25]

Propagations. To propagate $\chi(\mathbf{q}_H;t)$ in eq 11, we use the grid methods described by Kosloff and Kosloff.[41−43] In this approach, the wave function is represented on a three-dimensional grid of evenly spaced points. The advantage of this technique is that we can use fast Fourier transforms to transform between configuration space and momentum space, where the potential and kinetic energy operators are multiplicative, respectively. Using this method, we approximate

$$\chi(\mathbf{q}_H;t+\Delta t) = \exp\left[-\frac{i\Delta t}{\hbar}\hat{H}\right]\chi(\mathbf{q}_H;t) \tag{12}$$

with a Lanczos recursion scheme.[44,45] We find that 10 iterations are sufficient to propagate the wave function accurately and efficiently over the short time step already required by the time dependence of V^{eff}.

Due to the heavier mass and slower motions of the chlorine atoms, $\phi(q_{Cl};t)$ is approximated by a semiclassical Gaussian. Following Heller,[46] we take

$$\phi(q_{Cl};t) = \exp\left\{\frac{i}{\hbar}[\alpha_t(q_{Cl}-q_t)^2 + p_t(q_{Cl}-q_t) + \gamma_t]\right\} \tag{13}$$

Here, q_t and p_t provide the centers of the Gaussian in coordinate and momentum space, and the imaginary parts of α_t and γ_t describe the width and normalization of the Gaussian, respectively. If a locally harmonic approximation to the potential is employed,

$$V^{eff}(q_{Cl},t) \approx V(q_t) + V'(q_t)\,(q_{Cl}-q_t) + \frac{V''(q_t)}{2}(q_{Cl}-q_t)^2 \tag{14}$$

analytical expressions for the time derivatives of the parameters q_t, p_t, α_t, and γ_t in terms of V, V', and V'' can be derived,[46] and q_t, p_t, α_t, and γ_t are propagated using a Gear integrator.[47]

Approximation to the TDSCF Potential. One of the greatest challenges in implementing the TDSCF approximation comes in evaluating V^{eff} in eq 10. Because V^{eff} is time-dependent, this multi-dimensional integral must be evaluated at every time step. While this may not be difficult to do for small systems, for larger systems this becomes impractical. Several approaches have been proposed that reduce the computational load of the evaluations of V^{eff}.[30,48] In the present work, we assume that because the Q/SC TDSCF approximation requires a locally quadratic expansion of the potential in q_{Cl} around the center of the Gaussian q_t, we can use a quartic polynomial expansion in q_{Cl} to approximate the potential over longer times. This approach is similar to the multiple time step methods that have been applied to a variety of problems.[47] Specifically, if at $t = 0$, $\phi(q_{Cl};t)$ is centered at $q_{Cl}^{(0)}$, we approximate the potential for Ar_n(ClHCl) by

$$V = V^{inter}_{Ar_n(ClHCl)} + V^{LEPS}_{ClHCl} \approx \sum_{n=0}^{4}\frac{1}{n!}\left[\frac{\partial^n V}{\partial q_{Cl}^n}\right]_{q_{Cl}^{(0)}}(q_{Cl}-q_{Cl}^{(0)})^n \tag{15}$$

where the required derivatives are evaluated analytically at each of the grid points used in the quantum simulation. The expansion in eq 15 provides a good approximation to the potential so long as $|q_{Cl}^{(0)} - q_t|$ is small. Therefore, when this difference exceeds 0.01 Å we set $q_{Cl}^{(0)}$ equal to q_t and evaluate the derivatives in eq 15 with respect to the new $q_{Cl}^{(0)}$. More frequent updating of the derivatives does not affect the results reported below.

Numerical Details. We approximate the initial wave function as a $3N - 6$ dimensional Gaussian ($3N - 5$ when no argon atoms are present) which corresponds to the ground state of $Ar_n(ClHCl^-)$, and we assume a vertical transition to the excited state. The quantum wave function is propagated on a three-dimensional grid, the extent of which is defined by the HCl bond length. The grid spans −350 to 350 in q_{H_z}, and −150 to 150 in q_{H_x} and q_{H_y}, with 120 points in q_{H_z} and 50 in q_{H_x} and q_{H_y}. The semiclassical Gaussian wave function is centered at q_0 and $p_0 = 0$, with $\alpha_0 = i\hbar\omega_{Cl/2}$ and $\mathrm{Im}(\gamma_0)$ chosen to ensure that the wave function is normalized at $t = 0$.

Results and Discussion

The Dynamics. As a first step in our investigation of the effects of microsolvation on the Cl+HCl transition state dynamics, we look at how slices through the probability density, $|\chi(\mathbf{q}_H)|^2$, in the $q_{H_x}q_{H_z}$ and $q_{H_y}q_{H_z}$ planes are affected by the introduction of one or more argon argon atoms. When no argon atoms are present, the short time transition state dynamics involves the hydrogen atom moving away from the Cl−Cl axis and the probability density spreading around the chlorine atoms. Classically, this corresponds to the hydrogen atom orbiting around one of the chlorine atoms, forming HCl with nonzero angular momentum. Since this system is cylindrically symmetric, slices through the wave function will be independent of the plane in which they are plotted, as long as it contains the Cl−Cl axis.

In Figure 2, we plot slices through $|\chi(\mathbf{q}_H)|^2$ in the $q_{H_x}q_{H_z}$ and $q_{H_y}q_{H_z}$ planes for Ar_3(ClHCl) when $t = 24$ (a and b) and $t = 48$ fs (c and d). As is shown in the sketches in Figure 1, in this coordinate system the argon atoms lie in the xy plane, with $y > 0$ and symmetrically arranged with respect to the yz plane. Therefore, the slices in the $q_{H_x}q_{H_z}$ plane are symmetric. On the other hand, the slices in the $q_{H_y}q_{H_z}$ plane contain less amplitude at positive values of q_{H_y}, the half-plane where the argon atoms are located, than for negative values of q_{H_y}. The slices through the wave function in Figure 2 clearly demonstrate that the presence of the argon atoms leads to a decrease in probability amplitude near the location of the argon atoms, and an increase in probability amplitude in the regions of space furthest away from the argon atoms. Plots for the systems with $n = 1$, 2, 4, and 5 display similar trends, with the argon atoms blocking the hydrogen atom from orbiting around the chlorine atoms. In the case when there are four or five argon atoms, this orbiting motion is almost entirely blocked and the hydrogen atom becomes trapped near the Cl−H−Cl configuration.

Comparisons of the dynamics of the different sized clusters can be made more easily by comparing projections of the probability amplitude onto the $q_{H_x}q_{H_y}$ plane, the plane that is perpendicular to the Cl−Cl axis and on which all of the argon

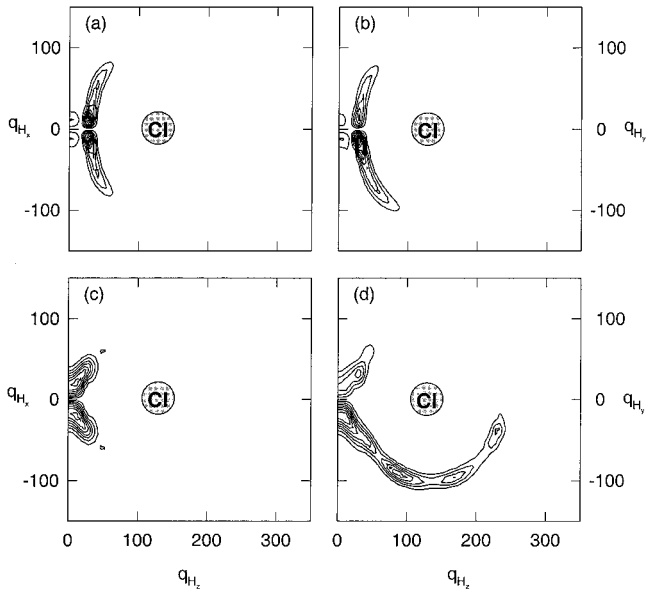

Figure 2. (a) and (c) Slices through $|\chi(\mathbf{q}_H;t)|^2 q_{H_x}$ are plotted in the $q_{H_x}q_{H_z}$, and (b) and (d) slices through $|\chi(\mathbf{q}_H;t)|^2 q_{H_y}$ are plotted in the $q_{H_y}q_{H_z}$, planes for the $Ar_3(ClHCl)$ system after 24 fs (a and b) and 48 fs (c and d). The argon atoms lie in the $q_{H_x}q_{H_y}$ plane, at positive values of q_{Hy}.

atoms lie. Such a comparison is made for $t = 48$ fs in Figure 3. We have indicated the approximate location of the argon atoms to facilitate the discussion that follows. As was stated above, the probability distribution for the $n = 0$ system is cylindrically symmetric. The addition of one argon atom produces a hole in the wave function in the region of the argon atom. This hole is a result of the short-range Ar−H repulsion. As the number of argon atoms is increased, the amount of configuration space that is available for the hydrogen atom to orbit around the chlorine atoms is reduced dramatically, because the Ar−Ar distance is small enough to prevent most of the probability amplitude from escaping between the argon atoms. When $n =$ 4 or 5, the symmetry of the arrangement of the argon atoms allows them to trap the hydrogen atom in a three-dimensional box, the sides of which are determined by the locations of the argon and chlorine atoms. Finally, there are small side peaks in the probability amplitudes at the edges closest to the location of the argon atoms when $n \leq 3$. These result from the longer range Ar−H attractive interaction.

In all of the plots in Figure 3, the probability amplitude can be divided into two parts, that which is localized near the origin and that which lies in a ring around the Cl−Cl axis with a radius of approximately 100. These two regions are most easily seen when $n = 0$, 1, or 5, but persists when $n = 2$, 3, and 4. Physically, the two regions correspond to the part of the wave packet that is trapped between the chlorine atoms and that which is orbiting around them. To quantify this effect, we calculate the fraction of the probability amplitude that is trapped in the center of the complex as a function of time, for each cluster size. This is shown graphically in Figure 4. Here, we define a three-dimensional cylinder, centered on the center of the ClHCl axis, with $\sqrt{q_{H_x}^2 + q_{H_y}^2} = 90$ and $|q_{H_z}| = 75$. In Figure 4, we plot the fraction of the probability amplitude that is enclosed by this cylinder as a function of time. The qualitative picture is insensitive to the precise dimensions of the cylinder. The parameters used here were chosen to minimize oscillations in the curves, plotted in Figure 4, that are caused by breathing of the trapped part of the wave packet.

The curves plotted in Figure 4 can be separated into three groups. When $n = 0$, most of the wave function has moved outside of the boundaries of the cylinder after 60 fs, indicating that the hydrogen atom is essentially free to rotate out of the center of the cluster. In the intermediate case when $n = 1$, 2, or 3, more of the wave function is trapped, although not completely. Finally, when $n = 4$ or 5, the hydrogen atom is almost entirely trapped. In this case, the probability of the hydrogen atom being outside of the cylinder remains less than 20% after 60 fs.

Based on these observations, as the cluster size is increased the ClHCl becomes forced to dissociate in a linear configuration. This is also reflected in Figure 5, which shows the time dependence of R_{ClCl} as a function of cluster size. We see that the rate of separation of the chlorine atoms increases as argon

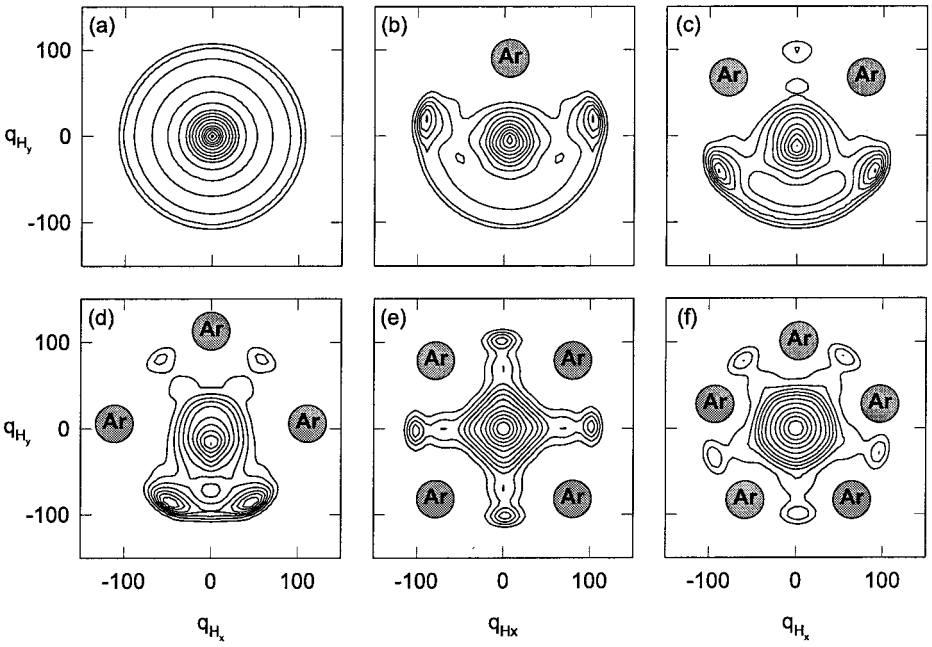

Figure 3. Projections of the probability amplitude $|\chi(\mathbf{q}_H;t)|^2$ after 48 fs of propagation, onto the $q_{H_x}q_{H_y}$ plane for (a) $n = 0$, (b) $n = 1$, (c) $n = 2$, (d) $n = 3$, (e) $n = 4$, and (f) $n = 5$. Qualitative positions of the argon atoms are labeled.

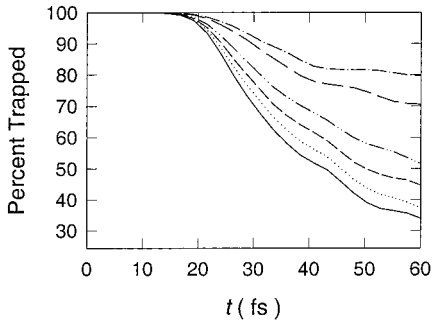

Figure 4. The fraction of the total wave function that is trapped between the chlorine atoms is plotted as a function of time for $n = 0$ (solid line), $n = 1$ (dotted line), $n = 2$ (short dashed line), $n = 3$ (dot−dot−dash line), $n = 4$ (long dashed line), and $n = 5$ (dot−dash line).

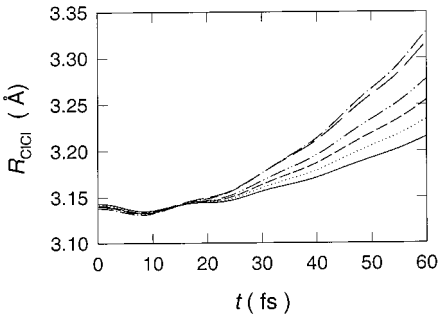

Figure 5. The time dependence of the R_{ClCl} for $n = 0$ (solid line), $n = 1$ (dotted line), $n = 2$ (short dashed line), $n = 3$ (dot−dot−dash line), $n = 4$ (long dashed line), and $n = 5$ (dot−dash line).

atoms are added to the cluster. When $n \leq 3$, the rate of the Cl−Cl separation increases linearly with cluster size. The increase in rate is largest when the fourth argon atom is introduced and remains approximately constant between $n = 4$ and 5. This can again be explained by the trapping effect that the argon atoms have on the wave function. Because the hydrogen atom is trapped in the center of the cluster, energy transfer between the hydrogen and chlorine atoms is enhanced, causing the chlorine atoms to separate more rapidly.

The Spectrum. The argon atoms perturb the wave function by reducing the amount of configuration space that is available to the hydrogen atom. This is important for properties that correspond to the bending motions of ClHCl, but for highly averaged quantities the effects are less dramatic. For example, we calculate the correlation function by

$$\begin{aligned} C^{\mathrm{TDSCF}}(t) &= \langle \Psi^{\mathrm{TDSCF}}(t=0) | \Psi^{\mathrm{TDSCF}}(t) \rangle \\ &= \langle \chi(t=0) | \chi(t) \rangle \langle \phi(t=0) | \phi(t) \rangle \exp\left(\frac{i}{\hbar}\int_0^t \langle V \rangle(t')\mathrm{d}t'\right) \\ &= C_{\mathrm{H}}(t) C_{\mathrm{Cl}}(t) \exp\left(\frac{i}{\hbar}\int_0^t \langle V \rangle(t')\mathrm{d}t'\right) \end{aligned} \quad (16)$$

The squared magnitude of $C^{\mathrm{TDSCF}}(t)$ is plotted as a function of cluster size and time in Figure 6. As is indicated in eq 16, within the TDSCF approximation, the correlation function can be expressed as the product of a correlation function derived from the quantum wave packet and one that is obtained from the semiclassical Gaussian times a phase factor. While the short time dynamics and the oscillations in $C^{\mathrm{TDSCF}}(t)$ reflect the dynamics of the hydrogen atom, the damping of these oscillations at longer times reflects the dynamics of the chlorine atoms. Further, because the amount of energy that is transferred from the hydrogen atom to the chlorine atoms increases with cluster size, $C_{\mathrm{Cl}}(t)$ decays more rapidly for the larger clusters, as is

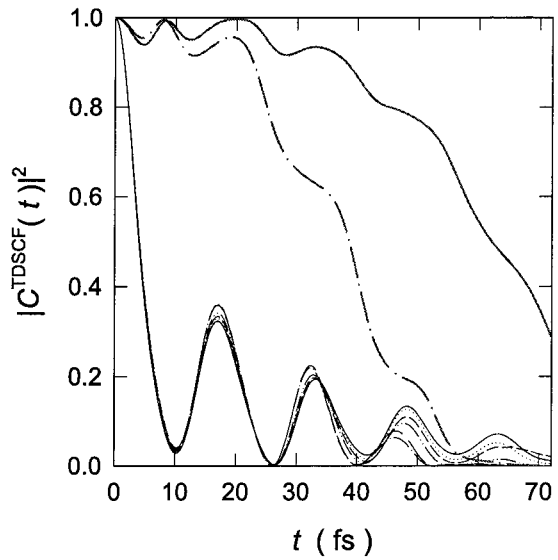

Figure 6. $|C^{\mathrm{TDSCF}}(t)|^2$ is plotted as a function of time and cluster size for $n = 0$ (solid line), $n = 1$ (dotted line), $n = 2$ (short dashed line), $n = 3$ (dot−dot−dash line), $n = 4$ (long dashed line), and $n = 5$ (dot−dash line). The semiclassical contribution to the correlation function is shown at the top of the plot for $n = 0$ and $n = 5$ (solid and dot−dash gray lines).

indicated by the curves plotted in gray in Figure 6. The correlation functions for the various cluster sizes are otherwise very similar, except for a slight change in frequency, which reflects changes in the frequencies associated with motion of the hydrogen atom perpendicular to the Cl−Cl axis.

The spectrum is obtained from the correlation function, using

$$I(E) \propto \frac{E}{\hbar}\int_{-\infty}^{\infty} \exp[i((E-E_0)t)/\hbar] C(t) \mathrm{e}^{-(t/1400)^2} \mathrm{d}t \quad (17)$$

where, E_0 is the zero-point energy of the anion and time is expressed in atomic units. The Gaussian provides a window function and is used to minimize the ringing in the spectrum that results from the fact that the propagations were run for no more than 72 fs.[49]

Given the similarities among the correlation functions, plotted in Figure 6, particularly at the shortest times, we expect that the structures of the calculated spectra will be very similar. This is indeed what we find. The most significant change in the spectra with increasing cluster size comes in the form of a blue shift of the origin, the magnitude of which is given by E_{sh} and is reported in Table 1. This blue-shift reflects a greater stabilization of $ClHCl^-$ with increasing cluster size compared to the stabilization of the neutral ClHCl.

The six calculated photoelectron spectra for $Ar_n(ClHCl^-)$ with $n = 0-5$ are plotted in Figure 7. They have been shifted by E_{sh} so that the origin bands occur at the same energy in order to facilitate comparisons among the spectra. In addition, we have fit all of the spectra to a set of six Gaussian bands. These have been plotted for the ClHCl system with dashed lines in Figure 7 and labeled with the letters **A** through **f**.

The calculated spectra agree well with previously reported spectra for ClHCl.[7,8,21] In the discussion that follows, we will use the notation of Chatfield et al.[24] and assign the bands with the pair of quantum numbers $[n_1,n_2]$, where n_1 and n_2 represent the number of quanta in q_{Hz} and the Cl−H−Cl bend, respectively.

For all cluster sizes, the [0,0] and [1,0] bands are the most intense. These bands are labeled **A** and **D**, respectively. As **D** corresponds to the state with one quantum in the mode in which

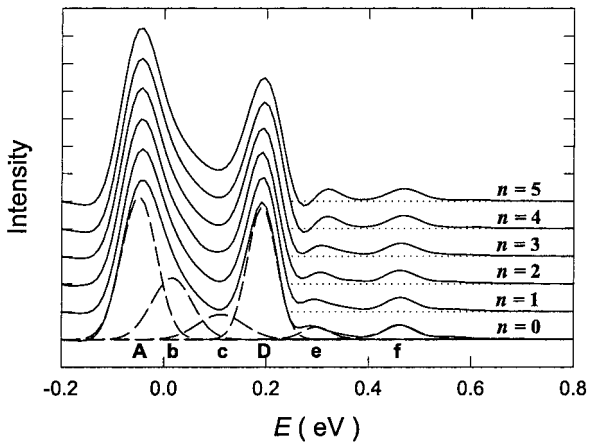

Figure 7. Plots of the calculated transition state spectra for $Ar_n(ClHCl^-)$ (solid lines), with $n = 0-5$. To facilitate comparison, the spectra for the systems with $n > 0$ have been shifted so that the origin band [A] lies at the same energy as that for $(ClHCl^-)$. The dashed lines represent a fit of the spectrum for $(ClHCl^-)$ to a sum of Gaussian bands, while the baselines for each of the spectra are plotted with dotted lines.

the hydrogen atom moves along the Cl−Cl bond axis, its position is insensitive to the introduction of the argon atoms in the plane perpendicular to this axis. However, the relative intensity of this band is sensitive to the number of argon atoms present. As the number of argon atoms is increased, $C^{TDSCF}(t)$ decays more rapidly. This results in fewer recurrences in the correlation functions, plotted in Figure 6 and the observed decrease in the intensity of **D** relative to **A** as more argon atoms are introduced.

The remaining four bands **b**, **c**, **e**, and **f** are much weaker and correspond to overtones in the bend and combination bands.[24] As such they correspond to motions in the plane perpendicular to the Cl−Cl axis. Since this is the plane that contains the argon atoms, the positions and intensities of these peaks are much more sensitive to the number of argon atoms than **A** or **D**. For example, as the number of argon atoms is increased, the shoulders on the blue side of band **A** and the red side of band **D** become more pronounced. These changes reflect increases in the intensities of **b** and **c** which have been previously assigned to overtones in the bend.[24] In addition, **e** shifts to the blue with increasing *n*. This band has been identified as the [1,2] band.

Finally, we find that there is a region of negative intensity between **D** and **e** when $n = 4$ or 5. This effect has been noted previously[40] and reflects the fact that there are important dynamical correlations between the hydrogen and chlorine motions that have been neglected in the TDSCF approximation. The increased importance of these couplings is a consequence of the increase in the amount of energy transferred from the hydrogen atom to the chlorine atoms with cluster size.

Summary and Conclusions

In this paper, we reported the results of an investigation of the effects of complex formation on the transition state dynamics of the Cl+HCl reaction. In particular, we have focused our study on how the transition state spectrum and the importance of the two dissociation channels are affected by cluster size. We find that as the number of argon atoms is increased from zero to five, the amount of configuration space that is available for the hydrogen atom to orbit around the chlorine atoms is reduced dramatically. Analysis of the wave functions shows that the argon atoms locally block the hydrogen atom from orbiting around the chlorine atoms, and, in the case when there are four or five argon atoms, this orbiting motion is essentially blocked and the hydrogen atom becomes trapped near the Cl−H−Cl configuration. When the hydrogen atom is trapped, the ClHCl is forced to dissociate in a linear configuration, rather than by the hydrogen atom rotating out of the center as it does in the unclustered system. In addition, enhanced energy transfer between the hydrogen and chlorine atoms causes the chlorine atoms to separate more rapidly as the cluster size increases.

The dominant effect that clustering has on the calculated spectrum is a blue shift in the overall spectrum. However, the effects on the features in the spectrum are much smaller. We see a small frequency shift to the blue and a small increase in intensity in the weaker bands that correspond to a progression in the bending modes. These are the modes that are most affected by clustering with argon atoms. However, because features that correspond to the stretching mode dominate the spectrum, a mode that is less strongly perturbed by the presence of the argon atoms, the overall spectrum is remains qualitatively unchanged. As such, we would expect that if instead of initiating the dynamics from the ground state of $Ar_n(ClHCl^-)$, the system is initiated with excitation in one of the bending modes the cluster size would have a larger effect on the spectroscopy.

Acknowledgment. The authors gratefully acknowledge the support from the National Science Foundation under Grant CHE-9732998 through the CAREER program, as well as an NSF predoctoral fellowship (H.B.L.). In addition, we acknowledge the Ohio State University Board of Regents and the Petroleum Research Fund, administered by the American Chemical Society, for partial support of this work.

References and Notes

(1) Miller, W. H. *Annu. Rev. Phys. Chem.* **1990**, *41*, 245.
(2) Manolopoulos, D. E.; Stark, K.; Werner, H.-J.; Arnold, D. W.; Neumark, D. M. *Science* **1993**, *262*, 1852.
(3) Bowman, J. M.; Schatz; G. C. *Annu. Rev. Phys. Chem.* **1995**, *46*, 169.
(4) Schatz; G. C. *J. Phys. Chem.* **1996**, *100*, 12839.
(5) Alexander, M. H.; Werner, H.-J.; Manolopoulos, D. E. *J. Chem. Phys.* **1998**, *109*, 5710.
(6) Continetti, R. E. *Int. Rev. Phys. Chem.* **1998**, *17*, 227.
(7) Metz, R. B.; Kitsopoulos, T. N.; Weaver, A.; Neumark, D. M. *J. Chem. Phys.* **1988**, *88*, 1463.
(8) Metz, R. B.; Weaver, A.; Bradforth, S. E.; Kitsopoulos, T. N.; Neumark, D. M. *J. Phys. Chem.* **1990**, *94*, 1377.
(9) Neumark, D. M. In *Advances in Molecular Vibrations and Collision Dynamics*; Bowman, J. M., Ratner, M. A., Ed.; JAI Press: Greenwich, CT, 1991; Vol. 1, 165.
(10) Neumark, D. M. *Annu. Rev. Phys. Chem.* **1992**, *43*, 153.
(11) Metz, R. B.; Bradforth, S. E.; Neumark, D. M. *Adv. Chem. Phys.* **1992**, *81*, 1.
(12) Yuexing, Z.; Yourshaw, I.; Reiser, G.; Arnold, C. C.; Neumark, D. M. *J. Chem. Phys.* **1994**, *101*, 6538.
(13) Arnold, D. W.; Bradforth, S. E.; Neumark, D. M. *J. Chem. Phys.* **1995**, *102*, 3493.
(14) Arnold, D. W.; Bradforth, S. E.; Neumark, D. M. *J. Chem. Phys.* **1995**, *102*, 3510.
(15) Bondi, D. K.; Connor, J. N. L.; Manz, J.; Römelt, J. *Mol. Phys.* **1983**, *50*, 467.
(16) Aziz, R. A.; Slaman, M. J. *Mol. Phys.* **1986**, *58*, 679.
(17) Botschwina, P.; Sebald, P.; Burmeister, R. *J. Chem. Phys.* **1988**, *88*, 5246.
(18) Hutson, J. M.; Beswick, J. A.; Halberstadt, N. *J. Chem. Phys.* **1989**, *90*, 1337.
(19) Burcl, R.; Cybulski, S. M.; Szczesniak, M. M.; Chalasinski, G. *J. Chem. Phys.* **1995**, *103*, 299.
(20) Gazdy, B.; Bowman, J. M. *J. Chem. Phys.* **1989**, *91*, 4615.
(21) Schatz; G. C. *J. Chem. Phys.* **1989**, *90*, 3582.
(22) Schatz; G. C.; Sokolovski, D.; Connor, J. N. L. *Faraday Discuss. Chem. Soc.* **1991**, *91*, 17.
(23) Hahn, O.; Gomez Llorente, J. M.; Taylor, H. S. *J. Chem. Phys.* **1991**, *94*, 2608.
(24) Chatfield, D. C.; Friedman, R. S.; Lynch, G. C.; Truhlar, D. G. *J. Phys. Chem.* **1992**, *96*, 57.

(25) McCoy, A. B.; Gerber, R. B.; Ratner, M. A. *J. Chem. Phys.* **1994**, *101*, 1975.
(26) Gerber, R. B.; Buch, V.; Ratner, M. A. *J. Chem. Phys.* **1982**, *77*, 3022.
(27) Gerber, R. B.; Ratner, M. A. *J. Phys. Chem.* **1988**, *92*, 3252.
(28) Alimi, R.; Garcia-Vela, A.; Gerber, R. B. *J. Chem. Phys.* **1992**, *96*, 2034.
(29) McCoy, A. B. In *Advances in Classical Trajectory Methods*; Hase, W. L., Ed.; JAI Press: Greenwich, CT, 1998; p 183.
(30) McCoy, A. B. *J. Chem. Phys.* **1995**, *103*, 986.
(31) Leitner, D. M.; Berry, R. S.; Whitnell, R. M. *J. Chem. Phys.* **1989**, *91*, 3470.
(32) Lennard-Jones, J. M.; Dent, B. M. *Trans. Faraday Soc. London* **1928**, *24*, 92.
(33) Hutson, J. M. *J. Chem. Phys.* **1988**, *89*, 4550.
(34) Watson, J. K. G. *Mol. Phys.* **1968**, *15*, 479.
(35) Alimi, R.; Gerber, R. B.; Hammerich, A. D.; Kosloff, R.; Ratner, M. A. *J. Chem. Phys.* **1990**, *93*, 6484.
(36) Gerber, R. B.; Buch, V.; Ratner, M. A. *Chem. Phys. Lett.* **1982**, *91*, 173.
(37) Manthe, U.; Meyer, H. D.; Cederbaum, L. S. *J. Chem. Phys.* **1992**, *97*, 9062.
(38) Fang; J.-Y.; Guo, H. *J. Chem. Phys.* **1994**, *101*, 1231.
(39) Wang, L.; McCoy, A. B. *PCCP* **1999**, *1*, 1227.
(40) McCoy, A. B. *Mol. Phys.* **1995**, *85*, 965.
(41) Kosloff, D.; Kosloff, R. *J. Comput. Phys.* **1983**, *52*, 35.
(42) Kosloff, R. *J. Phys. Chem.* **1988**, *92*, 2087.
(43) Kosloff, R. In *Dynamics of Molecules and Chemical Reactions*; Wyatt, R. E., Zhang, J. Z. H., Ed.; Marcel Dekker: New York, 1996; p 185.
(44) Park, T. J.; Light, J. C. *J. Chem. Phys.* **1986**, *852*, 5070.
(45) Leforestier, C.; Bisseling, R. H.; Cerjan, C.; Feit, M. D.; Friesner, R.; Guldberg, A.; Hammerich, A.; Jolicard, G.; Karrlein, W.; Meyer, H. D.; Lipkin, N.; Roncero, O.; Kosloff, R. *J. Comput. Phys.* **1991**, *94*, 59.
(46) Heller, E. J. *J. Chem. Phys.* **1975**, *62*, 1544.
(47) Allen, M. P.; Tidesley, D. J. *Computer Simulations of Liquids;* Clarendon Press: Oxford, 1987.
(48) Jungwirth, P.; Gerber, R. B. *J. Chem. Phys.* **1995**, *102*, 6046.
(49) Haug, K.; Metiu, H. *J. Chem. Phys.* **1992**, *97*, 4781.
(50) Note that $\alpha^{H} = 1.73$ Å^{-1}.